Domain-size statistics in the time-dependent Ginzburg-Landau equation driven by a dichotomous Markov noise

Katsuya Ouchi,[1,*] Naofumi Tsukamoto,[2] Takehiko Horita,[3,†] and Hirokazu Fujisaka[2]
[1]*Kobe Design University, 8-1-1 Gakuennishi-Machi, Nishi-ku, Kobe 651-2196, Japan*
[2]*Department of Applied Analysis and Complex Dynamical Systems, Graduate School of Informatics, Kyoto University, Kyoto 606-8501, Japan*
[3]*Department of Mathematical Sciences, Osaka Prefecture University, 1-1 Gakuencho, Osaka 599-8531, Japan*
(Received 31 August 2007; published 23 October 2007)

The domain dynamics of magnetization obeying the time-dependent Ginzburg-Landau equation driven by a dichotomous Markov noise is discussed. The system with various domain sizes in the early stage temporally evolves following an annihilation of neighboring domain walls, where each domain wall moves diffusively. Three statistics on the domain size, i.e., average domain size, the ensemble average of the domain size distribution function, and the spatial power spectrum of the magnetization, are evaluated to characterize the domain wall annihilation process. A phenomenological evolution equation for the domain-size distribution function is constructed by simplifying the annihilation process of the domain wall appropriately, and the underlying mechanism of those statistics is investigated.

DOI: 10.1103/PhysRevE.76.041129 PACS number(s): 64.60.-i, 02.50.-r, 05.40.-a

I. INTRODUCTION

Over the last decade, the dynamics of the magnetization of ferromagnetic systems below the critical temperature driven by a temporary oscillating external magnetic field has been extensively studied [1–4]. It has been established that the systems exhibit two qualitatively different dynamical phases according to the amplitude and frequency of the external field and experience a nonequilibrium transition between the two phases, which is called the *dynamical phase transition* (DPT). DPT was first observed numerically in the deterministic mean-field system [1], and has subsequently been studied in numerous Monte Carlo simulations of the kinetic Ising system [2]. It has also been observed experimentally in an ultrathin Co film on Cu(100) [3].

To elucidate the origin of DPT, Fujisaka *et al.* [4] proposed a simple model presented by

$$\dot{s} = f(s) + F(t), \tag{1}$$

where $f(s)=s-s^3$ and $F(t)=h\cos\Omega t$, and clarified that there exist two phases in Eq. (1) referred to as the *symmetry-restoring oscillation* (SRO) and the *symmetry-breaking oscillation* (SBO). They further investigated the spatially distributed system

$$\dot{s}(x,t) = s - s^3 + \nabla^2 s + F(t) \tag{2}$$

driven by the periodic field $F(t)=h\cos\Omega t$, and found that DPT studied with Eq. (2) belongs to the same universality class of the equilibrium Ising model in zero field.

It is quite interesting to ask whether DPT would be observed under other kinds of external fields, e.g., the dichotomous Markov noise (DMN). The dynamics of Eq. (1), with $F(t)$ being DMN and a nonlinear function $f(s)$, has been extensively studied by many authors mainly on the basis of the master equation [5]. For a review, see Ref. [6]. In Ref. [7], we studied Eq. (1) with $f(s)=s-s^3$ and DMN $F(t)$ with the amplitude H_0 in the context of DPT. It is established that the system exhibits two different behaviors called *symmetry-restoring motion* (SRM) for $H_0>H_c$, characterized by $\langle s(t)\rangle_T=0$, and *symmetry-breaking motion* (SBM) for $H_0<H_c$, characterized by the coexistence of two stable motions $\langle s_1(t)\rangle_T=-\langle s_2(t)\rangle_T\neq 0$, where $\langle\cdots\rangle_T$ is the long-time average, and H_c is the threshold of H_0 separating SRM from SBM. It should be noted that Eq. (1) with $F(t)$ being Gaussian white noise superposed on a periodic field is also an interesting subject of recent substantial studies [8], which is related to the study of thermal noise effect on DPT.

We are, now, interested in the dynamics of spatially distributed system $s(x,t)$ in one dimension obeying Eq. (2) driven by DMN $F(t)$ for $H_0<H_c$, instead of the periodically oscillating field. In general, $s(x,t)$, the order parameter at the position x and at time t, consists of many domains corresponding to each of the two SBMs separated by domain walls, and temporally evolves through a sequence of collisions and annihilations of the domain walls. The process was characterized by the distribution $n(l,t)$ of domains with size l, and we found that the ensemble average $\langle n(l,t)\rangle_F$ with respect to $F(t)$ obeys a power law $\langle n(l,t)\rangle_F \propto l^{-\beta}$ with $\beta\simeq 2$ [9]. The purpose of the present paper is to clarify the statistical characteristics of domain annihilation process by introducing several statistical quantities.

The present paper is organized as follows: In Sec. II, the system investigated in this paper is introduced, and the dynamics of a single domain wall is discussed. It is shown that the motion of the domain wall is diffusive. In Sec. III, the dynamics of domain walls is discussed by introducing the average domain size, the distribution of domain size, and the spatial power spectrum of $s(x,t)$. In Sec. IV, phenomenological evolution equations of the domain-size distribution are proposed in terms of partial differential equations driven by DMN, which are further reduced to a set of ordinary differ-

*ouchi@kobe-du.ac.jp
†horita@ms.osakafu-u.ac.jp

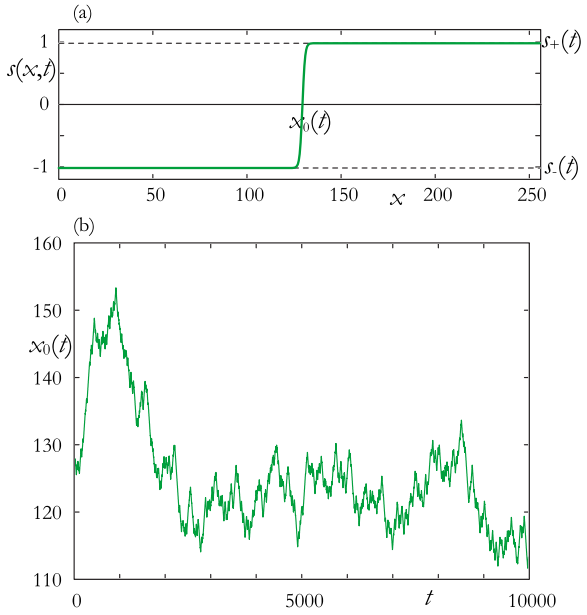

FIG. 1. (Color online) (a) Snapshot of $s(x,t)$ with a single domain wall at $x=x_0(t)$ and (b) time evolution of $x_0(t)$. The boundary conditions of $s(x,t)$ at time t are given by $s(+\infty,t)=s_+(t)$ and $s(-\infty,t)=s_-(t)$.

ential equations driven by DMN. In Sec. V, we attempt to find analytical forms of three statistical quantities discussed in Sec. III by using the reduced equations derived in Sec. IV. Concluding remarks are given in Sec. VI.

II. DYNAMICS OF A SINGLE DOMAIN WALL

We investigate the asymptotic dynamics of the spatially distributed order parameter $s(x,t)$ obeying Eq. (2), where $F(t)$ is DMN [6] which alternates between $+H_0$ and $-H_0$ with the transition rate τ_f^{-1}. The probability density $p(\tau)$ of the waiting time τ for the transitions of $F(t)$ is given by

$$p(\tau) = \tau_f^{-1} e^{-\tau/\tau_f}. \tag{3}$$

H_0 is set to be $H_0 < H_c$ throughout this paper, where $H_c = 2(1/3)^{3/2}$ is the critical value between SBM and SRM. Thus, the two stable uniform SBMs satisfying $s_+(t) > 0$ and $s_-(t) < 0$, which obey

$$\dot{s}_\pm(t) = s_\pm - s_\pm^3 + F(t), \tag{4}$$

coexist [7]. The existence of two SBMs implies that $s(x,t)$, in general, consists of more than two domains separated by domain walls.

Let us first consider the dynamics of a single domain wall in an infinite length of space. Figure 1(a) shows a domain wall locating at the position $x_0(t)$ at time t. The boundary condition $s(x,t)=s_\pm(t)$ for $x \to \pm\infty$ is set without loss of generality. We introduce an order parameter $a(x,t)$ defined by [4]

$$s(x,t) = \frac{1+a(x,t)}{2} s_+(t) + \frac{1-a(x,t)}{2} s_-(t), \tag{5}$$

which measures how much $s(x,t)$ is close to either $s_+(t)$ or $s_-(t)$. Substitution of Eq. (5) into Eq. (2) with using Eq. (4) yields

$$\dot{a}(x,t) = \xi(t)^2 (a - a^3) + \frac{\partial^2}{\partial x^2} a + \frac{3}{4}[s_+(t)^2 - s_-(t)^2](1 - a^2), \tag{6}$$

where $\xi(t)$ is given by

$$\xi(t) \equiv \frac{1}{2}[s_+(t) - s_-(t)]. \tag{7}$$

The boundary condition $a(x,t)=\pm 1$ for $x \to \pm\infty$ holds. Suppose $a_0(x,t)$ is the solution of

$$\dot{a}_0(x,t) = \xi(t)^2 (a_0 - a_0^3) + \frac{\partial^2}{\partial x^2} a_0 \tag{8}$$

satisfying $a_0(x,t) > 0$ (<0) for $x > 0$ (<0), and $a(x,t)$ can be approximated by $a(x,t)=a_0[x-x_0(t),t]$ where the domain wall locates $x=x_0(t)$. Here $x_0(t)$ is determined by

$$-\dot{x}_0 \frac{\partial}{\partial x} a_0 = \frac{3}{4}[s_+(t)^2 - s_-(t)^2](1 - a_0^2). \tag{9}$$

Multiplying each side of Eq. (9) by $\frac{\partial}{\partial x} a_0$ and integrating over x, one obtains the equation

$$\dot{x}_0(t) = -\frac{s_+(t)^2 - s_-(t)^2}{\sigma(t)}, \quad \sigma(t) \equiv \int_{-\infty}^{\infty} \left(\frac{\partial}{\partial x} a_0 \right)^2 dx. \tag{10}$$

We assume τ_f is large and employ an adiabatic approximation for $s_\pm(t)$. The stable fixed point s_{0+} (s_{0-}) of Eq. (4) with $F(t)=+H_0$ $[F(t)=-H_0]$, satisfying $s_{0\pm} > 0$, is given by

$$s_{0\pm} \equiv \cos\varphi \pm \frac{1}{\sqrt{3}} \sin\varphi, \tag{11}$$

where $\sin 3\varphi = H_0/H_c$ [7]. By the symmetry of the system, $-s_{0-}$ $(-s_{0+})$ is also the stable fixed point of Eq. (4) with $F(t)=+H_0$ $[F(t)=-H_0]$. By using the stable fixed points, $s_\pm(t)$ is approximated as

$$s_\pm(t) = \pm \frac{H_0 \pm F(t)}{2H_0} s_{0+} \pm \frac{H_0 \mp F(t)}{2H_0} s_{0-}. \tag{12}$$

Then ξ in Eq. (7) is given by the constant $\xi=\cos\varphi$. Thus, the stationary solution of $a_0(x,t)$ in Eq. (8) is obtained as

$$a_0(x) = \tanh(\xi x/\sqrt{2}), \tag{13}$$

which leads to $\sigma = 2\sqrt{2}\xi/3$. As a result, the position $x_0(t)$ of the domain wall obeys

$$\dot{x}_0 = v(t) = -\frac{V}{2} \tilde{F}(t), \tag{14}$$

where $V \equiv 2\sqrt{6} \sin\varphi$ and $\tilde{F}(t) \equiv F(t)/H_0$ are defined. Figure 1(b) shows a numerically evaluated time evolution of $x_0(t)$,

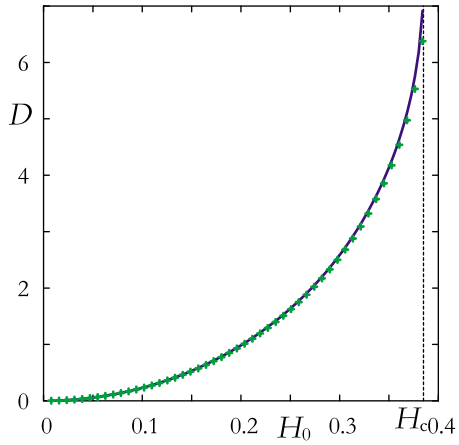

FIG. 2. (Color online) D vs H_0. Solid line shows the theoretical result given by Eq. (17). The symbols are the simulation results for $\tau_f=10$.

which indicates that the dynamics of the domain wall can be characterized by a diffusion process.

The diffusion constant D is estimated as follows: For a large τ_f, it is assumed that $v(t)$ satisfies the relations

$$\langle v(t)\rangle = 0, \quad \langle v(t_1)v(t_2)\rangle = \frac{V^2}{4}e^{-2\tau_f^{-1}|t_1-t_2|}. \tag{15}$$

The variance is obtained as

$$\langle [x_0(t)-x_0(0)]^2\rangle = \frac{V^2}{8}\tau_f[2t+\tau_f(e^{-2\tau_f^{-1}t}-1)] \simeq 2Dt \tag{16}$$

with the diffusion constant

$$D = \frac{V^2}{8}\tau_f. \tag{17}$$

Equation (17) is compared with the numerical simulation in Fig. 2. It reveals that the dynamics of an isolated domain wall is well approximated by a random walk if τ_f is large enough.

III. STATISTICS OF MANY DOMAIN WALLS

The spatial pattern of $s(x,t)$ starting with a random initial condition, in general, shows the coexistence of many domains with various domain sizes in the early stage and then shows a process of annihilations of neighboring domain walls in the temporal evolution, as shown in Fig. 3. We here examine the distribution $n(l,t)$ of domain size l, the time evolution of average domain size $\overline{l(t)}$, and spatial power spectrum $I(k,t)$ of $s(x,t)$ in order to characterize the domain wall annihilation process. All the results in this section are obtained by numerical integration of Eq. (2) for $H_0=0.38$ and $\tau_f=10$, where the Euler difference scheme with the time increment $\Delta t=0.01$, the space interval $\Delta x=0.5$, and the system size $L=2^{19}$ with a periodic boundary are used.

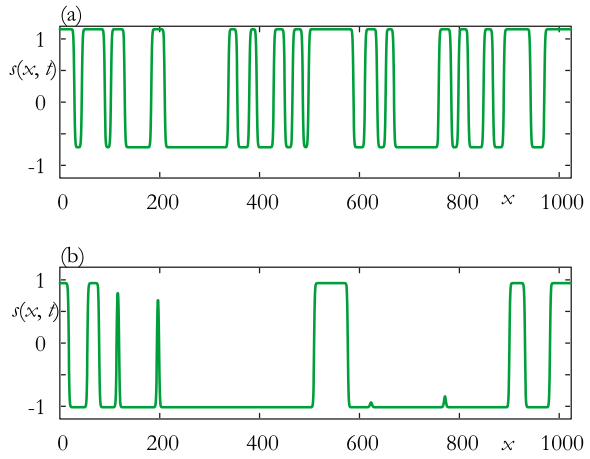

FIG. 3. (Color online) Spatial pattern of $s(x,t)$ for t= (a) 20 and (b) 35 with a lot of domains.

A. Distribution of domain size

The ensemble average of the distribution of domain size is defined as follows: A sample time series of DMN $F(t)$, which is called a realization, is numerically evaluated by applying a pseudo-random number generator. The realization gives a distribution function $n(l,t)$ of domain size l by integrating Eq. (2). Then the ith distribution function $n_i(l,t)$ for the ith realization of $F(t)$ is introduced. The ensemble average $\langle n(l,t)\rangle_F$ with respect to $F(t)$ is defined by

$$\langle n(l,t)\rangle_F \equiv \lim_{N_R\to\infty}\frac{1}{N_R}\sum_{i=1}^{N_R} n_i(l,t), \tag{18}$$

where N_R is the total number of realizations. Hereafter the ensemble average with respect to $F(t)$ is denoted by $\langle\cdots\rangle_F$.

Figure 4 shows a numerically evaluated $\langle n(l,t)\rangle_F$ as a function of l for several values of t. The initial state $s(x,0)$ in solving Eq. (2) for each realization is chosen to satisfy the condition that the values of $\int_0^\infty n_i(l,0)dl$ for all i are almost the same. The figure shows that the form of $\langle n(l,t)\rangle_F$ for

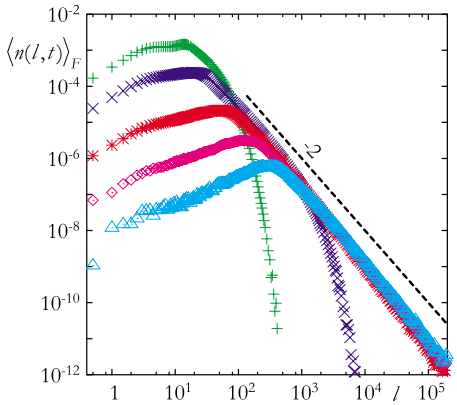

FIG. 4. (Color online) Time evolution of $\langle n(l,t)\rangle_F$ at t=4(+), 20(×), 100(*), 500(◇), and 2500(△). The dashed line shows l^{-2}.

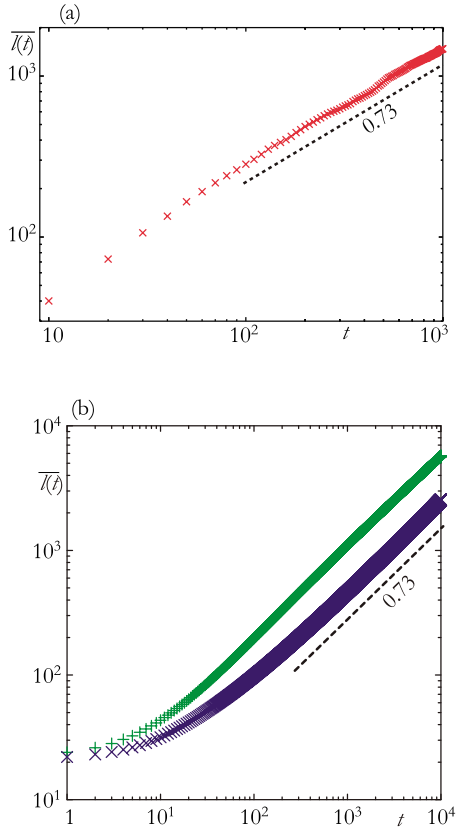

FIG. 5. (Color online) Time dependence of $\overline{l(t)}$ defined by Eq. (20): (a) the result obtained by numerical integration of Eq. (2), (b) the theoretical results obtained in Sec. V B by using Eq. (45) together with (+) the reduced equations for domain size [Eqs. (32), (34), and (35)], and with (×) Eqs. (46), (47), and (34).

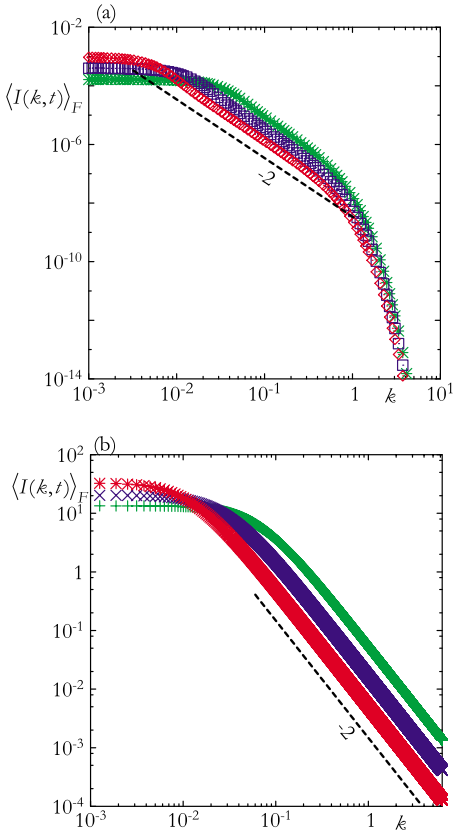

FIG. 6. (Color online) Time evolution of $\langle I(k,t)\rangle_F$ defined by Eq. (22): (a) the numerically obtained results by integrating Eq. (2) at $t=100(*)$, $500(\square)$, and $2500(\diamond)$, (b) the theoretical results at $t=100(+)$, $500(\times)$, $2500(*)$ discussed in Sec. V C.

$l \gg l_0(t)$, $l_0(t)$ denoting the peak position of $\langle n(l,t)\rangle_F$, changes from an exponential distribution to a power distribution

$$\langle n(l,t)\rangle_F \propto l^{-\beta} \tag{19}$$

with $\beta \simeq 2$ for a large t.

B. Temporal evolution of average domain size

The average domain size $\overline{l(t)}$ is defined by using $\langle n(l,t)\rangle_F$ as

$$\overline{l(t)} \equiv \frac{\int_0^\infty l\langle n(l,t)\rangle_F dl}{\int_0^\infty \langle n(l,t)\rangle_F dl}. \tag{20}$$

Equation (20) is numerically obtained by counting the numbers of domain walls in all the realizations. Figure 5(a), showing the dependence of $\overline{l(t)}$ on t, reveals that $\overline{l(t)}$ grows for large t as

$$\overline{l(t)} \propto t^{0.73}. \tag{21}$$

C. Spatial power spectrum

The ensemble average of the spatial power spectrum $\langle I(k,t)\rangle_F$ is then calculated to study the spatial correlation of $s(x,t)$, where $I(k,t)$ is defined by

$$I(k,t) \equiv \lim_{L\to\infty} \frac{1}{L}\left|\int_0^L s(x,t)e^{-ikx}dx\right|^2. \tag{22}$$

Figure 6(a) shows the numerically evaluated $\langle I(k,t)\rangle_F$ at several values of t. It is apparent that the ensemble average of the power spectrum is characterized by the Lorentzian form, i.e.,

$$\langle I(k,t)\rangle_F \propto \frac{\gamma(t)}{k^2+\gamma(t)^2}, \tag{23}$$

where $\gamma(t)$ is the inverse correlation length of the spatial correlation. One finds that $\gamma(t)$ decreases in time.

IV. PHENOMENOLOGICAL TIME EVOLUTION EQUATION FOR $n(l,t)$

In this section, we introduce a phenomenological time evolution equation for $n(l,t)$ to investigate the statistical properties described in Sec. III. We here consider a simplified model of the dynamics for the order parameter $a(x,t)$

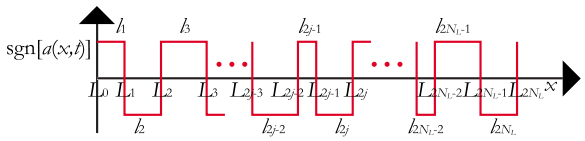

FIG. 7. (Color online) Spatial configuration at time t of the phenomenological model. The vertical axis represents $\mathrm{sgn}[a(x,t)]$. $l_j(t)$ and $L_j(t)=\Sigma_{k=1}^{j} l_k(t)$ denote the jth domain length and the jth domain wall position, respectively.

defined in Eq. (5) with a periodic boundary of the system size L. In this model, the spatial pattern is approximated by the sequence of $\mathrm{sgn}[a(x,t)]$, as shown in Fig. 7.

The model assumes that the system evolves temporally only through the motion of the domain walls. Each domain size at time t is denoted as $l_j(t)$ with $j=1,2,\ldots,2N_L(t)$, where $N_L(t)$ is the total number of domains in the $a(x,t)>0$ region, which is called the "+" side. $N_L(t)$ is also equal to the number of domains in the $a(x,t)<0$ region (the "−" side) due to the periodic boundary condition. The number densities $n_{\pm}(l,t)$ of the domains with size l for "±" sides are defined by

$$n_+(l,t) \equiv \lim_{L\to\infty} \frac{1}{L} \sum_{j=1}^{N_L(t)} \delta[l_{2j-1}(t) - l], \tag{24a}$$

$$n_-(l,t) \equiv \lim_{L\to\infty} \frac{1}{L} \sum_{j=1}^{N_L(t)} \delta[l_{2j}(t) - l], \tag{24b}$$

where the limit is taken by keeping $N_L(0)/L$ constant. One finds that the conditions $\lim_{l\to-0} n_{\pm}(l,t)=\lim_{l\to\infty} n_{\pm}(l,t)=0$ are satisfied.

We construct phenomenological evolution equations of $n_{\pm}(l,t)$ as follows. In the case that no domain walls collide, we assume that the growth rate of all of the shrinking domains takes $-V$ and that of the stretching domains takes $+V$, where V is the same as that in Eq. (14). Thus, $l_j(t)$ obeys the equation of motion

$$dl_j(t)/dt = (-1)^j V\tilde{F}(t), \tag{25}$$

$[j=1, 2, \ldots, 2N_L(t)]$. From Eqs. (24) and (25), one obtains the equations of $n_{\pm}(l,t)$ as

$$\dot{n}_{\pm}(l,t) = \pm \tilde{F}(t) \frac{\partial n_{\pm}(l,t)}{\partial l}, \tag{26}$$

where the notation $\dot{g} \equiv (1/V) dg/dt$ is introduced.

Equations (26) are the starting equations to study the collision process of domain walls. In the case of $\tilde{F}(t)=+1$, the "+" side domains shrink, and the equation for $n_+(l,t)$ is unchanged, where the collision process is included by the condition $\lim_{l\to-0} n_+(l,t)=0$. The equation of motion for $n_-(l,t)$ for the stretching domains is, on the other hand, derived as follows. If a "+" side domain, say $(2j-1)$th domain, disappears due to the collision of two neighboring domain walls, then the neighboring "−" side domains of $(2j-2)$th and $(2j)$th coalesce into a new "−" side domain with the size $l'_{2j-2}(t)=l_{2j-2}(t)+l_{2j}(t)$, (See Fig. 7). The probability of realization of such a process per unit time and unit system size is equal to the probability of the disappearance of a "+" side domain per unit time and unit system size, which is equal to $Vn_+(0,t)$. The time evolution equation for $n_-(l,t)$ with $\tilde{F}(t)=+1$ is, therefore, given by

$$\dot{n}_-(l,t) = \alpha_+(t) \left[-2n_-(l,t) + \frac{1}{N(t)} n_- * n_-(l,t) \right] - \tilde{F}(t) \frac{\partial n_-(l,t)}{\partial l}, \tag{27}$$

where $\alpha_+(t) \equiv n_+(0,t)/N(t)$ and

$$N(t) \equiv \int_0^\infty n_+(l,t) dl = \lim_{L\to\infty} \frac{N_L(t)}{L} \tag{28}$$

is the number density for total "+" side domains. It should be noted that $N(t)$ is also equal to the number density for total "−" side because of the periodic boundary condition. In Eq. (27), the terms including $-2n_-(l,t)$ and the convolution $n_-*n_-(l,t) \equiv \int_0^l n_-(l',t) n_-(l-l',t) dl'$ express the annihilation and creation of domains by the coalescence of two domains, respectively. By the symmetry of the system, the time evolution equations for $n_{\pm}(l,t)$ including both $\tilde{F}(t)=+1$ and -1 are summarized as

$$\dot{n}_{\pm}(l,t) = \alpha_{\mp}(t) \left[-2n_{\pm}(l,t) + \frac{1}{N(t)} n_{\pm} * n_{\pm}(l,t) \right] \pm \tilde{F}(t) \frac{\partial n_{\pm}(l,t)}{\partial l} \tag{29}$$

with

$$\alpha_{\pm}(t) = n_{\pm}(0,t)/N(t). \tag{30}$$

It should be noted that $\alpha_+(t)$ $[\alpha_-(t)]$ always vanishes if $F(t)=+1$ $[F(t)=-1]$ because of Eqs. (26).

The solutions of (29) are asymptotically approximated by the exponential forms [9]

$$n_{\pm}(l,t) \simeq \frac{N(t)}{l_c^{\pm}(t)} \exp\left[-\frac{l - l_{\pm}(t)}{l_c^{\pm}(t)} \right] \theta[l - l_{\pm}(t)] \tag{31}$$

with the Heaviside function $\theta(x)$. $l_c^{\pm}(t)$ in Eq. (31) are the widths of $n_{\pm}(l,t)$ and obey the equations of motion given by

$$\dot{l}_c^{\pm}(t) = \frac{l_c^{\pm}(t) + l_{\pm}(t)}{l_c^{\mp}(t)} \Delta[l_{\mp}(t)], \tag{32}$$

where $\Delta(x)$ is the function defined by

$$\Delta(x) = \begin{cases} 0, & x > 0 \\ 1, & x = 0. \end{cases} \tag{33}$$

$l_{\pm}(t)$ in Eqs. (31) and (32) are the shortest domain sizes for the "±" sides and obey the equations of motion given by

$$\dot{l}_{\pm}(t) = \mp \tilde{F}(t) + \Delta[l_{\pm}(t)], \tag{34}$$

with $l_{\pm} \geq 0$. The number density of either "+" or "−" side domains, $N(t)$, is determined by

$$1 = N(t)[l_c^+(t) + l_c^-(t) + l_+(t) + l_-(t)], \tag{35}$$

which is the result from the trivial condition that the system size L is invariant under the time evolution. Equations (31), (32), (34), and (35) are fundamental equations to discuss the coalescing process and are referred to as the *reduced equations for domain size*. It has been confirmed numerically that each number density $n_\pm(l,t)$ for each realization is characterized by the exponential form given in Eq. (31) [9].

V. ANALYSIS FOR STATISTICS OF DOMAIN WALLS

In this section, we attempt to derive Eq. (19) with $\beta=2$, Eq. (21), and Eq. (23) by using the reduced equations for domain size. Let us introduce an assumption that $l_c^\pm(t)$ and $l_\pm(t)$ with sufficiently large t satisfy the condition of either $l_c^+(t) \gg \{l_c^-(t), l_\pm(t)\}$ or $l_c^-(t) \gg \{l_c^+(t), l_\pm(t)\}$, depending on each realization. The condition due to Eqs. (32) and (34), i.e., the exponential time dependence of $l_c^\pm(t)$ and the diffusive time dependence of $l_\pm(t)$, is referred to as *the long-time condition*.

A. Power law in the domain-size distribution

Let us discuss the distribution of domain size and try to derive the power-law dependence Eq. (19) by using the long-time condition. By replacing the symbol "+"("−") with "g" in the former (latter) case of the long-time condition, and simultaneously "−"("+") with "s", the condition is expressed as $l_c^g(t) \gg \{l_c^s(t), l_g(t), l_s(t)\}$.

We first consider the region $l \gg \{l_\pm(t)\}$. In this case, $\theta(l - l_\pm(t))=1$ and $l - l_\pm(t) \simeq l$ hold in Eqs. (31). Therefore, $n(l,t)$ for $l \gg \{l_\pm(t)\}$ is written as

$$n(l,t) \simeq \frac{1}{l_c^g(t)}\left[\frac{1}{l_c^g(t)} e^{-l/l_c^g(t)} + \frac{1}{l_c^s(t)} e^{-l/l_c^s(t)}\right], \tag{36}$$

where the approximation $N(t) \simeq 1/l_c^g(t)$ has been used. In the range $l > l_c^s \ln(l_c^g/l_c^s)$, the second term in rhs of Eq. (36) can be neglected by noting $l_c^g \gg l_c^s$. The ensemble average of Eq. (36) is, therefore, given in the form

$$\langle n(l,t)\rangle_F \simeq \left\langle \frac{1}{l_c^g(t)^2} e^{-l/l_c^g(t)} \right\rangle_F = \int_0^\infty l_c^{-2} e^{-l/l_c} p(l_c,t) dl_c, \tag{37}$$

where $p(l_c,t)$ is defined by

$$p(l_c,t) \equiv \langle \delta[l_c^g(t) - l_c]\rangle_F. \tag{38}$$

The distribution function $p(l_c,t)$ of $l_c^g(t)$ is estimated as follows. For $l_c^s(t)$, Eq. (32) implies

$$\dot{l}_c^s(t) = \frac{l_c^s(t) + l_s(t)}{l_c^g(t)} \Delta[l_g(t)] \simeq 0 \tag{39}$$

because of $l_c^g \gg l_c^s$. Namely, $l_c^s(t)$ is almost constant in this approximation. On the other hand, ignoring $l_g(t)$, Eq. (32) for $l_c^g(t)$ is integrated to yield

$$\ln \frac{l_c^g(t)}{l_c^g(0)} \simeq \frac{V}{l_c^s} \int_0^t \Delta[l_s(u)] du, \tag{40}$$

where l_c^s is approximated to be constant. The equation of motion of $l_s(u)$ is given by Eq. (34), which is a kind of random walk with a barrier at the origin. Hence, the integral in the rhs of Eq. (40) is evaluated by measuring the duration τ that $l_s(u)$ stays at the origin for $0 < u < t$. The probability density $P(\tau;t)$ of τ defined by

$$P(\tau;t)d\tau \equiv \text{Prob}\left\{\tau < \int_0^t \Delta[l_s(u)] du < \tau + d\tau\right\} \tag{41}$$

is approximately derived for $t \gg \tau_f$ in the form

$$P(\tau;t) \simeq \sqrt{\frac{2}{\pi \tau_f t}} e^{-\tau^2/(2\tau_f t)}, \tag{42}$$

as shown in Appendix A.

Equation (42) gives the probability density that $\frac{l_c^s}{V} \ln \frac{l_c}{l_c(0)}$ takes the value τ at time t, and thus the probability density $p(l_c,t)$ for $t \gg \tau_f$ is evaluated as

$$p(l_c,t) \simeq \sqrt{\frac{2}{\pi \tau_f t}} \frac{l_c^s}{V l_c} e^{-\left[\frac{l_c^s}{V} \ln \frac{l_c}{l_c(0)}\right]^2/(2\tau_f t)} \propto t^{-1/2} \frac{1}{l_c}. \tag{43}$$

The ensemble average in Eq. (37) is eventually written as

$$\langle n(l,t)\rangle_F \propto t^{-1/2} \int_0^\infty e^{-l/l_c} l_c^{-3} dl_c = t^{-1/2} l^{-2}, \tag{44}$$

together with Eq. (38). As shown in Fig. 8, the l_c dependence of Eq. (43) is confirmed by solving the reduced equations for domain size and also by solving the original system Eq. (2).

B. Time evolution of average domain size

Since $\int_0^\infty l[n_+(l,t) + n_-(l,t)] dl = 1$ and $\int_0^\infty [n_+(l,t) + n_-(l,t)] dl = 2N(t)$, the definition of $\overline{l(t)}$ in Eq. (20) is rewritten as

$$\overline{l(t)} = \frac{1}{2\langle N(t)\rangle_F}. \tag{45}$$

If one assumes the long-time condition, Eq. (32) is approximated by $\dot{l}_c^\pm(t) = [l_c^\pm(t)/l_c^\mp(t)]\Delta(l_\mp(t))$, or equivalently by

$$\dot{x}_\pm = e^{-x_\mp} \Delta[l_\mp(t)], \tag{46}$$

where $x_\pm \equiv \ln l_c^\pm$ are introduced. Therefore $N(t)$ defined by Eq. (35) is approximated as

$$N(t) \simeq \frac{1}{e^{x_+(t)} + e^{x_-(t)}}. \tag{47}$$

As a result, the average domain size $\overline{l(t)}$ with the long-time condition is obtained by using Eq. (47) in Eq. (45).

Time evolution of Eq. (45) is numerically examined by obtaining $N(t)$ both from the reduced equations for domain size and from Eq. (47) with Eqs. (46) and (34). The results are shown in Fig. 5(b). It is revealed that both the reduced

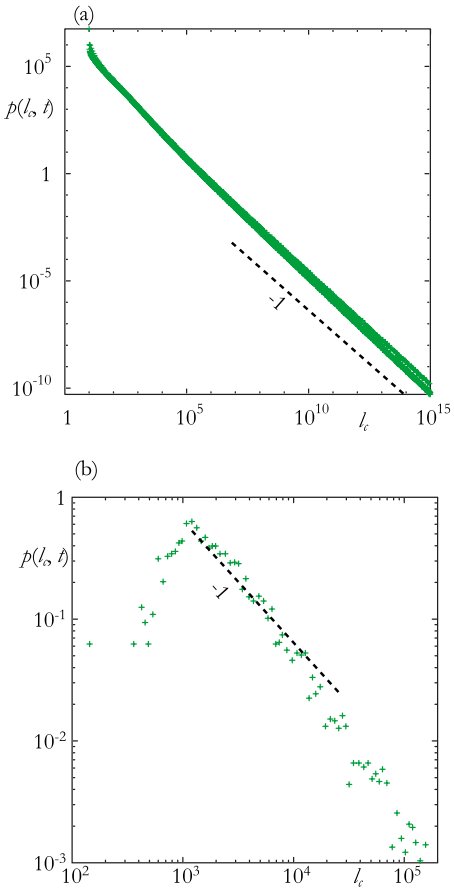

FIG. 8. (Color online) Distributions $p(l_c,t)$ defined by Eq. (38); (a) the result obtained by using a numerical integration of the reduced equations for domain size [Eqs. (32) and (34)] and (b) the result obtained by using a numerical simulation of Eq. (2).

equations for domain size and their simplified equations obtained by applying the long-time condition lead to the same time dependence Eq. (21) as that obtained from Eq. (2).

We should note the following point. If $N(t)$ is approximated as $N(t) \simeq 1/l_c^g(t)$ with $l_c^g(t)$ satisfying Eq. (40), then $\langle N(t)\rangle_F$ for $t \gg \tau_f$ is evaluated, by using Eq. (42), as

$$\langle N(t)\rangle_F = \frac{1}{l_c^g(0)}\sqrt{\frac{2}{\pi\tau_f t}}\int_0^t e^{-\tau^2/2\tau_f t}e^{-V\tau/l_c^s}d\tau$$

$$\simeq \frac{l_c^s}{Vl_c^g(0)}\sqrt{\frac{2}{\pi\tau_f t}}[1-e^{-(1/2\tau_f+V/l_c^s)t}] \propto t^{-1/2}. \quad (48)$$

Equation (48) contradicts the results mentioned above, so that the approximation of Eq. (39) seems not to be appropriate for the derivation of $\overline{l(t)}$. The simultaneous differential equations (46) have to be solved in this case.

C. Spatial power spectrum

In this subsection, we derive the spatial power spectrum $I(k,t)$ defined by Eq. (22) for the phenomenological model, where the spatial pattern $a(x,t)$ at time t is approximated as a sequence of two values +1 and −1, i.e.,

$$a(x,t) = (-1)^n \quad (49)$$

for $L_n(t) < x < L_{n+1}(t)$ with $n = 0, 1, \ldots, 2N_L(t)-1$ (See Fig. 7). As shown in Appendix B, the power spectrum for the above pattern is obtained as

$$I(k,t) = \frac{8N(t)}{k^2}\,\mathrm{Re}\frac{[1-\alpha_+(k,t)][1-\alpha_-(k,t)]}{1-\alpha_+(k,t)\alpha_-(k,t)} \quad (50)$$

for $k > 0$, where $\alpha_\pm(k,t)$ are the characteristic functions defined by

$$\alpha_\pm(k,t) \equiv N(t)^{-1}\int_0^\infty e^{-ikl}n_\pm(l,t)dl. \quad (51)$$

By applying the approximate solutions (31), $\alpha_\pm$ are obtained as

$$\alpha_\pm = \frac{e^{-ikl_\pm(t)}}{1+ikl_c^\pm(t)}. \quad (52)$$

With Eq. (52), Eq. (50) yields

$$\langle I(k,t)\rangle_F = \frac{8}{k^2}\left\langle N(t)\frac{[a_+(t)a_-(t)-b_+(t)b_-(t)]c(t)+[a_-(t)b_+(t)+a_+(t)b_-(t)]d(t)}{c(t)^2+d(t)^2}\right\rangle_F, \quad (53)$$

where $a_\pm(t)$, $b_\pm(t)$, $c(t)$, and $d(t)$ are defined by

$$a_\pm(t) \equiv 1-\cos kl_\pm(t), \quad (54)$$

$$b_\pm(t) \equiv kl_c^\pm(t)+\sin kl_\pm(t), \quad (55)$$

$$c(t) \equiv 1-l_c^+(t)l_c^-(t)k^2-\cos k[l_+(t)+l_-(t)], \quad (56)$$

$$d(t) \equiv k\left[l_c^+(t)+l_c^-(t)\right]+\sin k[l_+(t)+l_-(t)]. \quad (57)$$

Under the long-time condition, Eq. (53) is reduced to

$$\langle I(k,t)\rangle_F \simeq \left\langle \frac{8N(t)}{k^2+\left(\frac{1}{l_c^+}+\frac{1}{l_c^-}\right)^2}\right\rangle_F. \quad (58)$$

The reduced equations for domain size are numerically integrated to determine the time dependence of $l_c^\pm(t)$. Equation

(58) is drawn in Fig. 6, where $N(t) \simeq [l_c^+(t)+l_c^-(t)]^{-1}$ is used. It can be found that the theoretical $\langle I(k,t)\rangle_F$ [Eq. (58)] is approximately given by the Lorentzian form and is in agreement with the simulation result.

VI. CONCLUDING REMARKS

In this paper, we investigated the dynamics of domain walls under the dichotomous Markov noise (DMN), particularly focusing on the spatial pattern of $s(x,t)$ under the condition that two stable uniform motions coexist. We first discussed the dynamics of a single domain wall for infinite system size. The equation of motion for the domain wall position $x_0(t)$ was derived, and it was found that the motion of $x_0(t)$ is characterized by the diffusion process.

The temporal evolution of $s(x,t)$ for a random initial condition was, then, discussed. In the early stage there exist many domains with various sizes and then the field $s(x,t)$ temporally evolves by repeating pair annihilation of neighboring domain walls. We introduced the distribution function $n(l,t)$ of domains with the size l to discuss the statistical characteristics of the process. The time evolution of its average value $\langle n(l,t)\rangle_F$ with respect to the applied DMN $F(t)$ was numerically evaluated, and it was found that $\langle n(l,t)\rangle_F$ change from an exponential distribution to a power distribution

$$\langle n(l,t)\rangle_F \propto l^{-\beta}, \tag{59}$$

with $\beta \simeq 2$ as time goes on. The average domain size $\overline{l(t)}$ defined by Eq. (20) was then investigated, and we found that the time dependence is given as

$$\overline{l(t)} \simeq t^{0.73}. \tag{60}$$

Furthermore, the spatial power spectrum $\langle I(k,t)\rangle_F$ was calculated to discuss the spatial correlation of $s(x,t)$. It was found that $\langle I(k,t)\rangle_F$ approximately takes the Lorentzian form with the line width $\gamma(t)$ which is a decreasing function of t. We proposed a phenomenological time evolution equation of $n(l,t)$ to discuss the mechanism for such statistics. It was eventually revealed that the power distribution of domain size l obtained after the ensemble average is due to the fact that the exponent of the exponential domain size distribution for each realization of $F(t)$ is given by a log-normal distribution. A set of simplified evolution equations to reproduce the time dependence of $\overline{l(t)}$ was derived. Nevertheless, we could not explain the time dependence [Eq. (60)] analytically because the nonlinear simultaneous differential equations given by Eq. (46) must be solved. The analytical form of the spatial power spectrum was finally derived, which is represented as the superposition of Lorentzians.

ACKNOWLEDGMENTS

This study was partially supported by a Grant-in-Aid for Scientific Research (C) of the Ministry of Education, Culture, Sports, Science, and Technology, (No. 19540401) and the 21st Century COE Program "Center Of Excellence for Research and Education on Complex Functional Mechanical Systems" at Kyoto University.

APPENDIX A: DERIVATION OF EQ. (42)

We consider the motion of $l_s(t)$ obeying the equation $\dot{l}_s(t)=\tilde{F}(t)+\Delta[l_s(t)]$ with the initial condition $l_s(0)=0$ and $\tilde{F}(0)=-1$. Let $P(\tau;t)d\tau$ be the probability that $\tau < \int_0^t \Delta[l_s(u)]du < \tau+d\tau$ with respect to all the possible paths of $\{l_s(u)\}$ based on realizations of $\{\tilde{F}(u)\}$. The probability density $P(\tau;t)$ can be decomposed into the sum

$$P(\tau;t) = \sum_{n=0}^{\infty} P^{(n)}(\tau;t), \tag{A1}$$

where $P^{(n)}(\tau;t)$ denotes the same probability density as $P(\tau;t)$ under the additional condition that $l_s(u)$ returns n times back to $l_s=0$ for $0<u<t$. Let $\rho_r(t)$ be the probability density of the recurrence time for the process $\{x(t)\}$ obeying

$$\frac{dx}{dt} = V\tilde{F}(t), \tag{A2}$$

i.e., dichotomous diffusion on a line. Then $P^{(n)}(\tau,t)$ $(n \geq 1)$ satisfies the recursion relation

$$P^{(n+1)}(\tau;t) = \int_0^{\tau} du \int_0^{t-\tau} ds \rho_r(s)p(u)P^{(n)}(\tau-u;t-s), \tag{A3}$$

where $P^{(0)}(\tau;t)$ is given by

$$P^{(0)}(\tau;t) = p^{(0)}(\tau)q^{(0)}(t-\tau) \tag{A4}$$

with $p^{(0)}(t) \equiv p(t)$, which is defined in Eq. (3), and

$$q^{(0)}(t) \equiv \int_t^{\infty} \rho_r(s)ds. \tag{A5}$$

By putting

$$P^{(n)}(\tau;t) = p^{(n)}(\tau)q^{(n)}(t-\tau), \tag{A6}$$

Equation (A3) is reduced to the recursion relations

$$p^{(n+1)}(t) = \int_0^t du p(u)p^{(n)}(t-u), \tag{A7a}$$

$$q^{(n+1)}(t) = \int_0^t du \rho_r(u)q^{(n)}(t-u), \tag{A7b}$$

with $P^{(n+1)}(\tau;t)=p^{(n+1)}(\tau)q^{(n+1)}(t-\tau)$. The Laplace-transform (LT) of Eq. (A6) for both τ and t is written as

$$\tilde{P}^{(n)}(z;Z) = \int_0^{\infty} dt \int_0^{\infty} d\tau e^{-Zt-z\tau}P^{(n)}(\tau;t) = \tilde{p}^{(n)}(z+Z)\tilde{q}^{(n)}(Z), \tag{A8}$$

where $\tilde{g}(z)$ represents the LT of $g(t)$. The LTs of Eqs. (A7) read

$$\tilde{q}^{(n)}(z) = [\tilde{\rho}_r(z)]^n\tilde{q}^{(0)}(z), \quad \tilde{p}^{(n)}(z) = [\tilde{p}(z)]^{n+1}. \tag{A9}$$

Substitution of Eqs. (A8) and (A9) into Eq. (A1) yields

$$\tilde{P}(z;Z) = \frac{1}{Z}\frac{[1-\tilde{\rho}_r(Z)]\tilde{\rho}_r(Z)\tilde{p}(z+Z)}{1-\tilde{\rho}_r(Z)\tilde{p}(z+Z)}, \tag{A10}$$

where the LT of Eq. (A5), $\tilde{q}^{(0)}(Z)=Z^{-1}[1-\tilde{\rho}_r(Z)]$, is introduced. The LT of Eq. (3) leads to

$$\tilde{p}(z) = \frac{1}{1+\tau_f z}. \tag{A11}$$

By substituting Eq. (A11) into Eq. (A10) and then applying the inverse LT with respect to z, one obtains the equation

$$\tilde{P}(\tau;Z) = \frac{[1-\tilde{\rho}_r(Z)]\tilde{\rho}_r(Z)}{\tau_f Z} e^{-(1+\tau_f Z-\tilde{\rho}_r(Z))\tau/\tau_f}. \tag{A12}$$

The explicit form of $\tilde{\rho}_r(Z)$ is derived as follows. The distribution function $f(x,t)$ for x obeying Eq. (A2) is obtained as shown in Ref. [10], where the initial condition is chosen as $f(x,0)=\delta(x)$ and $\frac{\partial f(x,t)}{\partial t}|_{t=0}=0$. Then the distribution at the origin $Q(t)\equiv f(0,t)$ is written in the form

$$Q(t) = V^{-1}e^{-t/\tau_f}\{\delta(t) + (2\tau_f)^{-1}[I_0(t/\tau_f) + I_1(t/\tau_f)]\}, \tag{A13}$$

where $I_\mu(z)$ are the modified Bessel functions of the first kind, and the corresponding $\tilde{Q}(z)$ is given by

$$\tilde{Q}(z) = \frac{1}{2V}\frac{z+2\tau_f^{-1}+\sqrt{z(z+2\tau_f^{-1})}}{\sqrt{z(z+2\tau_f^{-1})}}. \tag{A14}$$

Since $\tilde{\rho}_r(z)$ is related to $\tilde{Q}(z)$ as $\tilde{\rho}_r(z)=1-[V\tilde{Q}(z)]^{-1}$ because of $|dx/dt|=V$, one obtains

$$\tilde{\rho}_r(z) = 1+\tau_f z - \sqrt{\tau_f z(\tau_f z+2)}. \tag{A15}$$

Substituting Eq. (A15) into Eq. (A12) and expanding it, assuming $\tau_f Z \ll 1$ because we are interested in the case $t \gg \tau_f$, one finally gets

$$\tilde{P}(\tau;Z) = \sqrt{\frac{2}{\tau_f Z}} e^{-\sqrt{2\tau_f Z}\tau/\tau_f}. \tag{A16}$$

The inverse LT of Eq. (A16) with respect to Z yields Eq. (42).

APPENDIX B: DERIVATION OF EQ. (50)

Since the Fourier-transform of Eq. (49) is calculated as

$$\int_0^{L_{2N_L}} a(x,t)e^{-ikx}dx = \sum_{n=1}^{2N_L}(-1)^n \frac{1}{ik} e^{-ikL_{n-1}}(e^{-ikl_n}-1), \tag{B1}$$

$I(k,t)$ defined by Eq. (22) is written in the form

$$I(k,t) = \lim_{N_L\to\infty}\frac{2N(t)}{k^2}\mathrm{Re}\left[\frac{1}{N_L}\sum_{n=1}^{2N_L}(1-e^{-ikl_n}) + \frac{1}{N_L}\sum_{m=1}^{2N_L-1}\sum_{n=m+1}^{2N_L}(-1)^{n-m}e^{-ik\Sigma_{j=m+1}^{n-1}l_j}(e^{-ikl_n}-1)\times(1-e^{-ikl_m})\right], \tag{B2}$$

where $N(t)=N_L(t)/L_{2N_L}$ is used. By noting that the characteristic functions $\alpha_\pm(k,t)$ defined by Eq. (51) are expressed as $\alpha_+(k,t)=\lim_{N_L\to\infty}(1/N_L)\Sigma_{n=1}^{N_L}e^{-ikl_{2n-1}}$ and $\alpha_-(k,t)=\lim_{N_L\to\infty}(1/N_L)\Sigma_{n=1}^{N_L}e^{-ikl_{2n}}$, the first term of the rhs reduces to the form

$$\lim_{N_L\to\infty}\frac{1}{N_L}\sum_{n=1}^{N_L}[(1-e^{-ikl_{2n-1}})+(1-e^{-ikl_{2n}})] = (1-\alpha_+)+(1-\alpha_-). \tag{B3}$$

The second term can be rewritten as

$$\begin{aligned}
&\lim_{N_L\to\infty}\frac{1}{N_L}\sum_{n=1}^{N_L}(1-e^{-ikl_{2n-1}})(1-e^{-ikl_{2n}}) \\
&+\lim_{N_L\to\infty}\sum_{m=1}^{N_L-1}\frac{1}{N_L}\sum_{n=1}^{N_L-m}\Bigg[(1-e^{-ikl_{2n-1}})(1-e^{-ikl_{2(n+m)}}) \\
&\times\prod_{k=0}^{m-1}e^{-ikl_{2(n+k)}}e^{-ikl_{2(n+k)+1}} - (1-e^{-ikl_{2n-1}})(1-e^{-ikl_{2(n+m)-1}}) \\
&\times e^{-ikl_{2n}}\prod_{k=1}^{m-1}e^{-ikl_{2(n+k)-1}}e^{-ikl_{2(n+k)}} + (1-e^{-ikl_{2n}}) \\
&\times(1-e^{-ikl_{2(n+m)-1}})\prod_{k=1}^{m-1}e^{-ikl_{2(n+k)-1}}e^{-ikl_{2(n+k)}} - (1-e^{-ikl_{2n}}) \\
&\times(1-e^{-ikl_{2(n+m)}})e^{-ikl_{2n+1}}\prod_{k=1}^{m-1}e^{-ikl_{2(n+k)}}e^{-ikl_{2(n+k)+1}}\Bigg].
\end{aligned} \tag{B4}$$

By using the assumption that l_n and l_m $(n\neq m)$ are statistically independent of each other, which is based on the randomness of the initial pattern $s(x,0)$, Eq. (B4) is reduced to

$$\begin{aligned}
&(1-\alpha_+)(1-\alpha_-)+[(1-\alpha_+)(1-\alpha_-)\alpha_+\alpha_- - (1-\alpha_+)^2\alpha_- \\
&-(1-\alpha_-)^2\alpha_+]\sum_{n=0}^{\infty}(\alpha_+\alpha_-)^n \\
&= \frac{2(1-\alpha_+)(1-\alpha_-)-(1-\alpha_+)^2\alpha_- -(1-\alpha_-)^2\alpha_+}{1-\alpha_+\alpha_-}
\end{aligned} \tag{B5}$$

because of $|\alpha_\pm|<1$ for $k>0$. The substitution of Eqs. (B3) and (B5) into Eq. (B2) leads to Eq. (50).

[1] T. Tomé and M. J. de Oliveira, Phys. Rev. A **41**, 4251 (1990); J. F. F. Menders and E. J. S. Large, J. Stat. Phys. **64**, 653 (1991).

[2] W. S. Lo and R. A. Pelcovits, Phys. Rev. A **42**, 7471 (1990); M. Acharyya, Phys. Rev. E **56**, 1234 (1997); **56**, 2407 (1997); **58**, 179 (1998); **59**, 218 (1999); S. W. Sides, P. A. Rikvold, and M. A. Novotny, Phys. Rev. Lett. **81**, 834 (1998); Phys. Rev. E **59**, 2710 (1999); P. A. Rikvold *et al.*, in *Computer Simulation Studies in Condensed Matter Physics XIII*, edited by D. P. Landau, S. P. Lewis, and H.-B. Schüttler (Springer, Berlin, 2000), pp. 105–119; G. Korniss, C. J. White, P. A. Rikvold, and M. A. Novotny, Phys. Rev. E **63**, 016120 (2000).

[3] Q. Jiang, H-N. Yang, and G-C. Wang, Phys. Rev. B **52**, 14911 (1995); J. Appl. Phys. **79**, 5122 (1996).

[4] H. Fujisaka, H. Tutu, and P. A. Rikvold, Phys. Rev. E **63**, 036109 (2001).

[5] W. Horsthemke and R. Lefever, in *Noise-Induced Transitions* (Springer, Berlin, 1984), Chap. 9; I. Bena, C. Van den Broeck, R. Kawai, and K. Lindenberg, Phys. Rev. E **68**, 041111 (2003); P. Hänggi and P. Riseborough, Phys. Rev. A **27**, 3379 (1983); C. Van den Broeck and P. Hänggi, *ibid.* **30**, 2730 (1984).

[6] I. Bena, Int. J. Mod. Phys. B **20**, 2825 (2006).

[7] K. Ouchi, T. Horita, and H. Fujisaka, Phys. Rev. E **74**, 031106 (2006)

[8] V. N. Smelyanskiy, M. I. Dykman, and B. Golding, Phys. Rev. Lett. **82**, 3193 (1999); J. Lehmann, P. Reimann, and P. Hanggi, *ibid.* **84**, 1639 (2000); R. S. Maier and D. L. Stein, *ibid.* **86**, 3942 (2001).

[9] K. Ouchi, N. Tsukamoto, H. Fujisaka, and T. Horita, J. Korean Phys. Soc. **50**, 201 (2007)

[10] V. Valakrishnan and S. Chaturvedi, Physica A **148**, 581 (1988)